



8<sup>th</sup> Manufacturing Engineering Society International Conference

# Design and development of a calibration artefact for length measurement system

F. J. Brosed<sup>a,\*</sup>, R. Acero<sup>a</sup>, S. Aguado<sup>b</sup>, M. Herrer<sup>a</sup>, J. J. Aguilar<sup>a</sup>, J. Santolaria<sup>a</sup>

<sup>a</sup>Design and Manufacturing Engineering Department, Universidad de Zaragoza, María Luna 3, Zaragoza 50018, Spain

\*email: [fjbrosed@unizar.es](mailto:fjbrosed@unizar.es)

<sup>b</sup>Centro Universitario de la Defensa, Academia General Militar, Crtra Huesca s/n, Zaragoza 50090, Spain

---

## Abstract

Due to accuracy requirements, robots and machine-tools need to be periodically verified and calibrated through associated verification systems that sometimes use extensible guidance systems. This work presents a reference artefact to evaluate the performance characteristics of different extensible precision guidance systems applicable to robot and machine tool verification. To this end, we present the design, modeling, manufacture and experimental validation of a reference artefact to evaluate the behavior of these extensible guidance systems. The system should be compatible with customized designed guides, as well as with commercial and existing telescopic guidance systems. An estimation of the uncertainty of the reference artefact is evaluated with a Monte Carlo simulation.

© 2019 The Authors. Published by Elsevier B.V.

This is an open access article under the CC BY-NC-ND license (<http://creativecommons.org/licenses/by-nc-nd/4.0/>)

Peer-review under responsibility of the scientific committee of the 8th Manufacturing Engineering Society International Conference

*Keywords:* calibration artifact; kinematic support; dimensional metrology; machine tool; length measurement

---

## 1. Introduction

Volumetric verification is a verification technique to improve the accuracy of machine tools (MTs) and robots based on indirect measurement [1]. It uses the combined effect of all geometric errors through a parameter identification process [2]. Many studies have been carried out for its application to coordinate measurement machines (CMMs) and machine tools (MTs) [3, 4]. The increasing implementation of this verification technique in the field of machine tool verification has led to the development of verification procedures that depend on different factors such as the type of machine, the non-geometric errors of the machine, the system and measurement technique applied, etc. [5]. The result of the equipment's verification is linked to the calibration of the measurement system used, procedure which is normally carried out in accordance with the applicable standards. This applies to measuring instruments

commonly used in volumetric verification such as laser trackers [6]. However, in some cases, the lack of guidelines or standards makes it necessary to develop internal calibration procedures and to use specific reference gauges [7, 8].

Therefore, this work presents the development of a reference artefact to calibrate extensible guidance systems used in machine tools and robots verification procedures. The reference artefact materializes several working positions and lengths with a fixed reference origin. The reference origin consists of a nest for a precision sphere and the working positions will include different nests with precision spheres and kinematic couplings. The mechanical repeatability of the reference artefact for the nests' positioning in the different working locations is achieved with kinematic couplings configuration of spheres and cylinders. The design of the artefact will also compensate the errors associated with its deflections [9, 10].

The paper is structured as follows. Firstly, the authors analyze the requirements of the design and the structure of the reference artefact. Secondly, it is performed an evaluation of the different gauge design proposals by means of a finite element simulation in Solid Edge. In this analysis, it is measured for each case the displacement generated in the gauge due to the loads application. Then, the design proposals selected are manufactured by 3D printing and these prototypes are used in the experimental testing and measured with a CMM. Finally, after optimizing the design with the feedback of simulation and experimental testing, the paper presents an uncertainty estimation of the designed calibration system.

## 2. Analysis of the requirements and initial 3D prototypes

The calibration artefact has to materialize the calibration positions for a length measurement instrument. The instrument consist of a system that measures the distance between two spheres. One of the spheres is fixed to the instrument and the other is fixed to the machine tool, robot or coordinate measuring machine under verification. As it can be seen in Fig. 1, the gauge is composed of a sphere (1) and a support (5) to hold the sphere fixed to the machine tool under verification (6), being both located at the edges of the artefact. Between both sides, there is an interferometer (2) to measure the different distances that will be materialized in the gauge. These different lengths are achieved with a telescopic system (3) that also assures the alignment of the interferometer and the retroreflector (6). The interferometer is located on the left side of the gauge closed to the fix sphere (1). The retroreflector will be located on the other side of the system close to the sphere fixed to the machine tool. The calibration artefact should be able to calibrate measurement instruments with a measurement range from 400 mm to 1600 mm (Max. and Min. in Fig.1). Once calibrated, the instrument will give the distance between the centres of the two spheres.

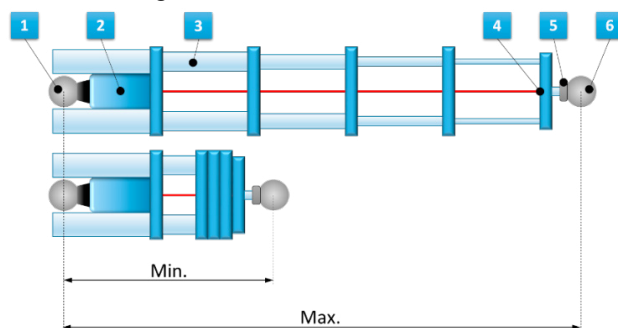


Fig. 1. Scheme and components of the measurement instrument. (1), sphere fixed to the instrument; (2) interferometer; (3) telescopic system; (4), retroreflector; (5) magnetic holder; (6) sphere fixed to the machine tool.

The calibration artefact has a fixed magnetic sphere-holder to lock the position of the sphere fixed to the instrument (1) and several kinematics supports to obtain a repeatable positioning of a sphere. When the sphere of the instrument (1) will be locked in the magnetic sphere holder and the other side of the instrument (5) will reach the sphere fixed to the machine tool, a calibrated length will be materialized in the gauge. The defined nominal lengths of the calibration artefact will range from 400 to 1600 mm.

During the calibration of the measurement instrument, the calibration artefact will rest in a flat surface. Therefore, the artefact will incorporate three support legs on its base to assure its stability in the calibration process.

The main components under analysis in the design of the gauge are the following: the position of the support points to minimize the deformation in the length measurement, the kinematic couplings support that will allow the movable sphere positioning with high repeatability and the mechanical structure to materialize the calibration lengths.

2.1. Kinematics supports

During the calibration of the measurement instrument, we need a repeatable positioning of the movable sphere to materialize the calibration positions. For this purpose, a kinematic base has been designed with calibrated spheres and cylinders (6-points 3-cylinders). The kinematic contact has two parts (upper and lower). In the lower part, six spheres are fixed in three pairs located at 120° meanwhile in the upper part, three cylinders are fixed with its axis located at 120° and pointing to the center of the geometrical distribution (Fig. 2). Each interface provides two constraints, totalling six constraints for the system. The best stability is achieved when the axis of the contact planes bisect the coupling triangle with each interface as a vertex of this triangle. Four spheres secure the position of the cylinders in the upper part. The upper and lower parts are fixed with magnets located in the centre of the geometrical distribution (in the upper and lower part respectively).

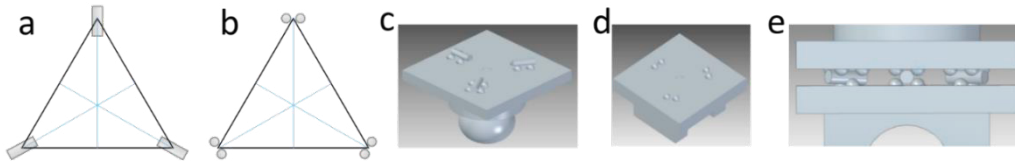


Fig. 2. Kinematic support for the mobile sphere. a) Distribution and orientation of the cylinders. b) Distribution and orientation of the spheres. c) Model of the cylinders fixed to the upper part. d) Model of the spheres fixed to the lower part. e) Model of the kinematic support mounted, contact between spheres and cylinders.

2.2. Calibration artefact structure

The main element of the artefact is a tube that goes through the other parts of the assembly. The junction between the tube and the other parts (magnetic holder or kinematic support for the magnetic holder) is materialized with a flange.

Two design proposals for the artefact structure are evaluated. The first prototype is a single bar structure in which the line of the measurement points is parallel to the bar and it is located beyond the structure (Fig. 3a). Each flange has been designed to hold the bar and locate the magnetic holder, in one case, and the kinematic support for the magnetic holder, in the rest of the cases, defining each measurement position (Fig. 3b and c).

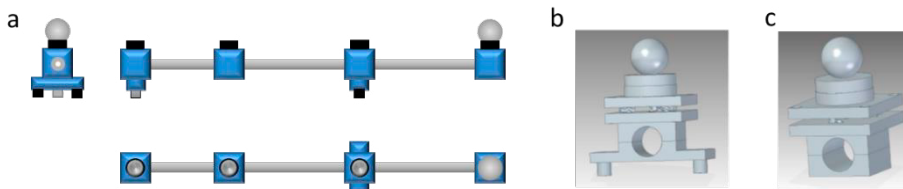


Fig. 3. a) Single bar structure for the calibration artefact. b) Flange of the single bar artefact with standing legs. c) Flange of the single bar artefact without standing legs.

The second prototype is a double bar structure that locates the line of the measurement points between both bars (Fig. 4a). The flanges hold the bars and support a base where the magnetic holder is located in the first point and the kinematic supports in the other cases (Fig. 4b). In the next subsection the location of the standing legs, Fig 4a and 4a, is discussed.

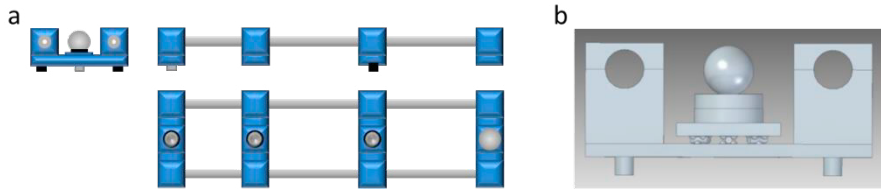


Fig. 4. a) Double bar structure for the calibration artefact to improve rigidity. b) Flange for the double bar structure with the base and kinematic support.

### 2.3. Air and Bessel support methodologies

A horizontal bar of great length requires two points of support in the direction of its length to be stable. The position of these standing legs determines the action of the gravity of this bar, since depending on how it is supported, measurement errors can be caused [11]. Therefore, if the supports are positioned at the ends it will warp in the center causing the ends to come closer and tilt upwards. On the contrary, if the two supports are positioned in the middle, the bar will be bent at the ends [9].

The distances between the supports of the bar have been defined using Airy and Bessel methodologies and comparing the results of the deformation. A bar supported at its Airy points has parallel ends and supported at its Bessel points has maximum length due to deflection reduction [10]. The distance between supports ( $a$ ) and the position of each support ( $L_{min}$  and  $L_{mid}$ ), for a simple bar of 1600 mm length ( $L$ ), appears in Table 1 and the deformation obtained in the bar appears in Fig 5.

Table 1. Values of the Airy and Bessel point.

	Airy	Bessel
$L$ [mm]	1600	1600
Factor	0.57735	0.55940
$a$ [mm]	923.76	895.04
$L_{min}$ [mm]	338.12	653.5
$L_{mid}$ [mm]	1261.88	1247.88

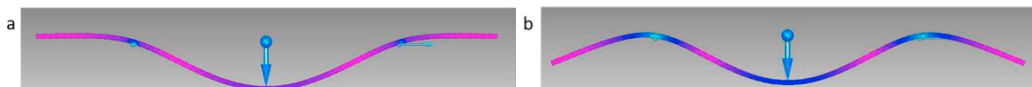


Fig. 5. Results of the simulation of a simple bar (aluminium) with two supports following each two methods. a) Simple bar supported at the Airy points. b) Simple bar supported at the Bessel points.

Four different positions of the supports are proposed, two of them following the Airy and Bessel methodologies. The other two configurations locate the supports in the reference flange (point 0, Fig. 6b) and in the flange that materialise  $L_{mid}$  (point 2, Fig. 6b) in the third case, and in the reference flange (point 0, Fig. 6c) and in the flange that materialise  $L_{max}$  (point 3, Fig. 6c) in the fourth case.

### 3. Design selection

In order to define the position of the standing legs a finite element analysis of the deformation of the structure has been carried out. The study analyses four different positions of the supports and the deformation occurred when the measurement system is placed in the three different measurement positions ( $L_{min}$ ,  $L_{mid}$  and  $L_{max}$ ). The measurement system will rest in the reference position and in the position under verification ( $L_{min}$ ,  $L_{mid}$  or  $L_{max}$ ). Therefore, in the analysis there is a load of 1N in the reference position (position of the magnetic holder, point 0, Fig. 6) and another load of the same value in the measurement position for each case. The four positions of the supports are the Airy point

( $a=923.76\text{mm}$ ), the Bessel points ( $a=895.04\text{mm}$ , Fig 6a), the supports located in the reference position and in the  $L_{mid}$  (Fig 6b) and finally the supports located in the reference position and in the  $L_{max}$  (Fig 6c).

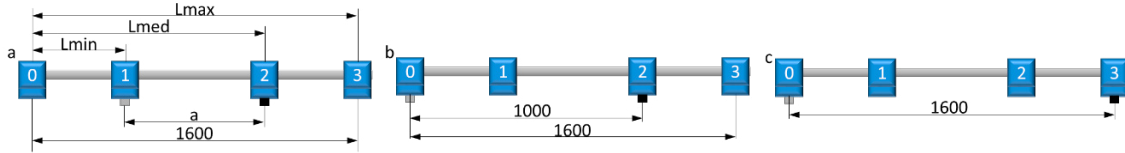


Fig. 6. Scheme of the four locations of the supports and the location of the loads in each simulation, there will be a load of 1N in point 0 for every simulation and another load of 1N in point 1 for the simulation of  $L_{min}$ , in point 2 for the simulation of  $L_{mid}$  and in point 3 for the simulation of  $L_{max}$ . a) Airy and Bessel points. b) Supports located in point 0 (reference) and in  $L_{mid}$ . c) Supports located in point 0 (reference) and in  $L_{max}$ .

The material properties taken in account for the structural analysis are shown in Table 2.

Table 2. Material Properties for Aluminium 6061, prototypes 1 and 2 and carbon fibre, prototype 3.

Property	Al 6061	Carbon fibre
Density [ $\text{T/m}^3$ ]	2.7	1.6
Young Module [GPa]	68.9	393.3
Poisson Coefficient	0.330	0.100

The increment of the measurement distance or the measurement error  $\Delta L_{MEAS}$  (1) characterises the deformation of the structure.

$$\Delta L_{MEAS} = \sqrt{(L_n + \Delta x_n - \Delta x_0)^2 + (\Delta y_n - \Delta y_0)^2 + (\Delta z_n - \Delta z_0)^2} \tag{1}$$

Where:  $L_n$  is the nominal distance of the measurement point ( $n=L_{min}$ ,  $L_{mid}$  and  $L_{max}$ );  $(\Delta x_n, \Delta y_n, \Delta z_n)$  are the displacements of the measurement point due to the deformation of the structure and  $(\Delta x_0, \Delta y_0, \Delta z_0)$  are the displacements of the reference point due to the deformation of the structure.

Combining the four proposed positions of the supports and the three different pairs of loads, twelve values of measurement error have been obtained for each prototype (Fig. 7).

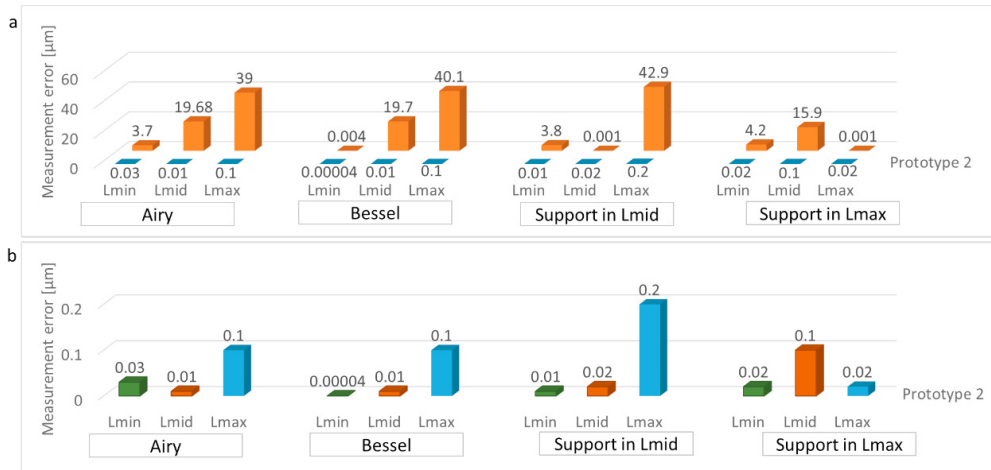


Fig. 7. a) Measurement error in  $\mu\text{m}$  for the twelve cases and the two prototypes. b) Detail of the results for the prototype 2.

The localization of the spheres beyond the structure line amplifies the measurement error due to the deformation in prototype 1. The measurement errors in prototype 2 are minimum using the Bessel points,  $0.1\mu\text{m}$  when the system is loaded in  $L_{max}$  position (points 0 and 3, Fig. 6) and lower in the other cases.

Finally, the kinematic supports have been tested manufacturing prototypes by additive manufacturing (Fig. 8a) and measuring the repeatability of the kinematic supports with the spheres and the cylinders. The repeatability of the kinematic supports has been measured with a Coordinate Measurement Machine (CMM). The position measurement repeatability of each location obtained after ten iterations was  $8\mu\text{m}$ .

Once the kinematic supports have been tested and the adequacy of the Bessel points for this application has been proved, we generated a new design with aluminium flanges and carbon fibre structure tubes (27'' diameter, 1830 mm length). The number of measurement points increments from three in the previous prototypes to seven (Table 3). In this case, the values of the measurement errors obtained for each measurement position are under  $0.1\mu\text{m}$ .

Table 3. Bessel and measurement points for prototype 3 (proposed nominal values).

A: $n=0$	B: $n=1$	Bessel 1	C: $n=2$	D: $n=3$	E: $n=4$	F: $n=5$	Bessel 2	G: $n=6$	H: $n=7$
0.00	280.00	396.54	535.00	785.00	1040.00	1295.00	1403.46	1545.00	1800.00
[mm]									

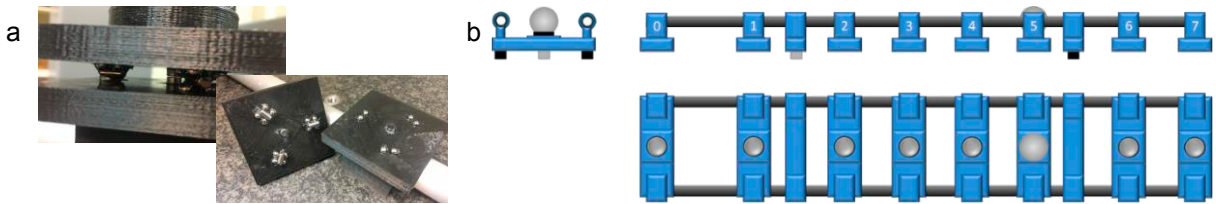


Fig. 8. a) Kinematic supports samples manufactured by additive manufacturing. b) Prototype 3.

#### 4. Manufacture, assembly, performance and results

The flanges, the bases where the kinematic supports are, and the standing legs of the artefact were made of Aluminium 6061 for the prototype 3. The flanges joint the carbon fibre tubes with the base that contains the magnetic holder for the position A ( $n=0$ , Fig. 8b) and with the base that contains the kinematic supports for the rest of the cases, positions B to H ( $n$  from 1 to 7, Fig. 8b).

The flanges geometry has been redesign to adequate it to a wire electroerosion manufacturing process (Fig.9a and b).

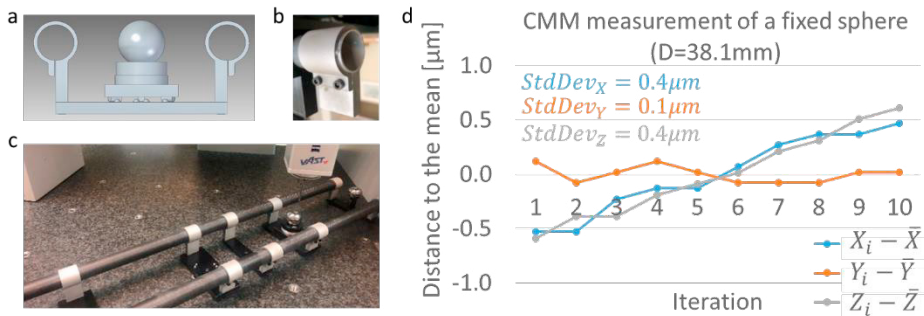


Fig. 9. a) Model of the flanges in prototype 3. b) Detail of the flange embracing a tube. c) Prototype 3 with the new flanges and the carbon fibre tubes during performance test in CMM. d) CMM measuring a fixed sphere (Diameter 38.1mm), distance to the mean of the ten iterations in mm and standard deviation of the sample x, Y and Z coordinates.

The position of the spheres has been measured with a Coordinate Measurement Machine (CMM) to obtain the uncertainty of the calibration artefact. First, the repeatability of the CMM measuring a sphere with a diameter of 38.1mm (1½'') has been estimated in  $0.4\mu\text{m}$ . The measurement position number 3 (Fig. 8b) was measured ten times with the CMM without removing the sphere from the kinematic support (Fig. 9d).

A second measurement with ten iterations was carried out assembling and disassembling the kinematic support with the sphere located in position number 3 (not fixed sphere, Fig. 10). The results are compared with those obtained

without removing the kinematic support (fixed sphere, Fig. 10).

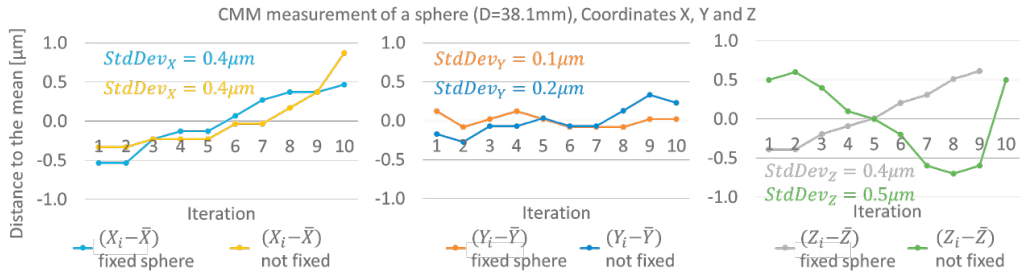


Fig. 10. CMM measuring a sphere (Diameter 38.1mm), distance to the mean of the ten iterations in mm and standard deviation of the sample in X coordinate, Y coordinate and Z coordinate. The results are compared with those obtained measuring a fixed sphere.

Z coordinate is more sensible to the movements when mounting and demounting the kinematic support but, in any case, the standard deviation of the sample is low enough for the application.

Once the repeatability of the kinematic support is checked, the next step is to verify the effect of the deformation in the measurement length corresponding to each sphere position. To accomplish this goal, the measurement of the reference position (A, number 0) and the others positions moving the kinematic support with the sphere from one position to another (from B, position number 1, to H, position number 7) has been carried out. This measurement procedure is repeated ten times. The results obtained allow estimating the repeatability of the measurement length in each position (Fig. 11a). This value is the input data for the simulation using the Monte Carlo method to estimate the uncertainty of the calibration artefact.

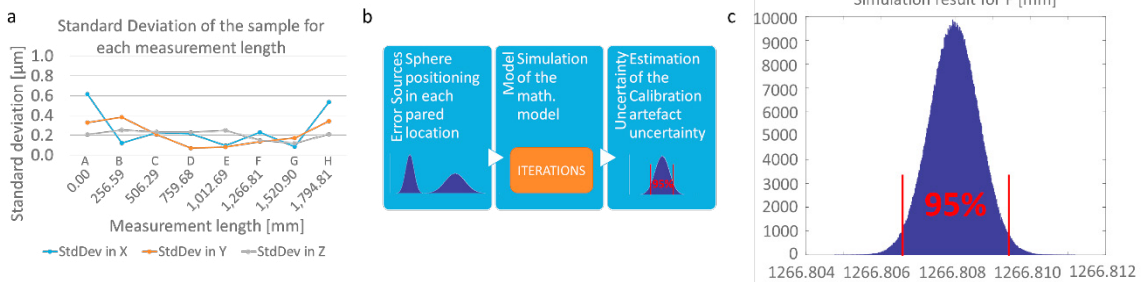


Fig. 11. a) CMM measuring a sphere (Diameter 38.1mm), in each position of the artefact. The graph shows the standard deviation of the sample (ten iterations) for each measurement length (X, Y and Z coordinates). The abscissae identify the mean value of the measurement length of each position (from A to H). b) Scheme of the uncertainty estimation using Monte Carlo Method. c) Monte Carlo simulation result for F, position number 5. Measurement length 1266.808 mm,  $U(k=2)=2.6\mu\text{m}$ .

The MC simulation can estimate the uncertainty of the reference artefact in the calibration of length measurement systems [12]. The input data for the MC simulation method are the probability distributions of the variability of the different error sources. In this case, the main error source is the variability of the positioning of each calibration point, being the distribution of this variability a normal distribution (Fig. 11b). The nominal value of each position coordinate is the mean value obtained from the CMM measurement. The standard deviation of the distribution of each position is also the standard deviation of the CMM measurements for each position. The results of the MC simulation are shown in Table 4 including the uncertainty for each length measurement. As an example, the uncertainty distribution for F position number 5 is shown in Fig. 11c. The uncertainty values have been calculated according with the GUM [13, 14] using a confidence level of 95% ( $k = 2$ ).

Table 4. Bessel and measurement points for prototype 3 (proposed nominal values).

Position	B	C	D	E	F	G	H
Number, n	1	2	3	4	5	6	7
Measurement length [mm]	256.586	506.29	759.684	1012.694	1266.808	1520.905	1794.811
Uncertainty (k=2) [mm]	0.0025	0.0026	0.0026	0.0024	0.0026	0.0024	0.0032

## 5. Conclusions

This work presented the design, manufacturing and experimental validation of a reference artefact to calibrate extensible guidance systems used in machine tools and robots verification procedures. It combines the use of spheres and spherical nests with kinematic supports that assure the high repeatability of the system. Different design proposals were evaluated with finite element analysis and two final prototypes were experimentally tested assuring that the design of kinematic couplings performs the expected function. The paper finally presents an uncertainty estimation of the calibration artifact using a Monte Carlo simulation.

## Acknowledgements

This research was funded by the Ministerio de Economía, Industria y Competitividad with project number Reto 2017 - DPI2017-90106-R, by Aragon Government (Department of Industry and Innovation) through the Research Activity Grant for research groups recognized by the Aragon Government (T56\_17R Manufacturing Engineering and Advanced Metrology Group) co-funded with European Union ERDF funds (European Regional Development Fund 2014-2020, “Construyendo Europa desde Aragón”) and by the Universidad de Zaragoza and the Centro Universitario de la Defensa, project number UZCUD2018-TEC-04.

## References

- [1] A.P. Longstaff, S. Fletcher, S. Parkinson, A. Myers, The role of measurement and modelling of machine tools in improving product quality, *Int. J. Metrol. Qual.*, 4 (2013) 177-184.
- [2] J.H. Jung, J.P. Choi, S.J. Lee, Machining accuracy enhancement by compensating for volumetric errors of a machine tool and on-machine measurement, *Journal of Materials Processing Technology*, 174 (2006) 56-66.
- [3] S. Aguado, J. Santolaria, D. Samper, J. Velazquez, and J. J. Aguilar, Empirical analysis of the efficient use of geometric error identification in a machine tool by tracking measurement techniques, *Meas. Sci. Technol.*, 27 (2016) 12pp.
- [4] Z. He, J. Fu, X. Zhang, and H. Shen, A uniform expression model for volumetric errors of machine tools, *Int. J. Mach. Tools Manuf.*, 100 (2016) 93–104.
- [5] S. Aguado, J. Santolaria, D. Samper, and J. J. Aguilar, Protocol for machine tool volumetric verification using commercial laser tracker, *Int. J. Adv. Manuf. Technol.*, 75 (2014) 425–444.
- [6] W. JingDong, G. JunJie, Research on volumetric error compensation for NC machine tool based on laser tracker measurement, *Technological Sciences*, 55 (2012) 3000-3009.
- [7] A. Hudlemeyer, D. Sawyer, C. J. Blackburn, V. D. Lee, M. Meuret, C. M. Shakarji, Considerations for Design and In-Situ Calibration of High Accuracy Length Artifacts for Field Testing of Laser Trackers, National Institute of Standards and Technology, March (2015). <https://www.nist.gov/publications/considerations-design-and-situ-calibration-high-accuracy-length-artifacts-field-testing> [Retrieved: 2018].
- [8] H. Zhao, L. Yu, H. Xia, W. Li, Y. Jiang, H. Jia, 3D artifact for calibrating kinematic parameters of articulated arm coordinate measuring machines, *Measurement Science and Technology*, 29 (2018) 8pp.
- [9] D. Sawyer, B. Parry, S. Phillips, C. Blackburn, B. Muralikrishnan, A model for geometry-dependent errors in length artefacts, *Journal of Research of the National Institute of Standards and Technology*, 117 (2012) 216-230.
- [10][5] J. Verdirame, Airy points, bessel points, minimum gravity sag and vibration nodal points of uniform beams, *Mechanics and Machines*, 2016. <http://www.mechanicsandmachines.com>. [Retrieved: 2018].
- [11] R. Köning, B. Przebierala, C. Weichert, J. Flügge, H. Bosse, A revised treatment of the influence of the sample support on the measurement of line scales and the consequences for its use to disseminate the unit of length, *Metrologia*, 46 (2009) 187-195.
- [12] P. Pérez, S. Aguado, J.A. Albajez, J. Santolaria, Influence of laser tracker noise on the uncertainty of machine tool volumetric verification using the Monte Carlo method, *Measurement*, 133 (2019) 81-90.,
- [13] BIPM; IEC; IFCC; ILAC; ISO; IUPAC; IUPAP; OIML, Evaluation of Measurement Data—Guide to the Expression of Uncertainty in Measurement, JCGM 100 Bureau International des Poids et Mesures (BIPM), 2008.
- [14] BIPM; IEC; IFCC; ILAC; ISO; IUPAC; IUPAP; OIML, Evaluation of Measurement Data—Supplement 1 to the Guide to the Expression of Uncertainty in Measurement—Propagation of Distributions Using a Monte Carlo Method, JCGM 101 Bureau International des Poids et Mesures (BIPM), 2008.